JOURNAL OF MATERIALS SCIENCE **34** (1999) 5593–5599

Dry sliding wear of an Al_2O_3 continuous fibre reinforced Al-Cu alloy against steel counterface

HUA-NAN LIU, KEISAKU OGI
Department of Materials Science and Engineering, Kyushu University, Hakozaki 6-10-1, Higashi-ku, Fukuoka 812-8581, Japan
E-mail: ogi@zaiko.kyushu-u.ac.jp

The tribological properties of Al_2O_3 continuous fibre reinforced Al-4.43 wt %Cu alloy composites with a fibres' volume fraction of about 0.55 were measured for five types of fibre orientations under a dry sliding contact with a bearing steel. Fibres were in a plain perpendicular to wear surface and parallel to sliding direction, and had the angles 0°, 45°, 90°, or 135° with respect to the direction of motion of the counterface; or were anti-parallel the sliding direction. The results show obvious dependence of wear characteristics on fibres orientation: for the 45°, 90°, and 135° orientations, the larger the fibres' angle, the lower the volume loss; while the 0° orientation resulted in a higher steady-state wear rate than those of the 45°, 90°, and 135°, orientations, except that the anti-parallel orientation caused the highest volume loss at all sliding distances. The wear mechanism was inferred as a oxidation-microgrooving process through the analyses of worn surface and subsurface with the aid of optical microscope and scanning electron microscope. Also it was found that the fibres' broken and subsurface deformation had played an important role in causing wear anisotropy.

1. Introduction

Metal matrix composites (MMCs) attract increasing attentions in both technological and commercial applications. Apart from high specific strength and stiffness, MMCs often possess excellent friction and wear properties. Nowadays, the Al_2O_3 or Al_2O_3-SiO2 discontinuous fibre reinforced Al alloy composites have been used commercially in the Toyota diesel engine pistons [1], crankshaft pulleys [2] and the Honda cylinders of aluminium engine blocks [3, 4, 5], to improve wear resistance. However, because of the complicity of the interrelationships among the different parameters involved in MMCs-metal couple tribological phenomena, the establishment of a formal model predicting wear rates of these tribosystems as a function of all tribological parameters was still out of reach [6], hence the detail studies on the factors related to MMCs tribological behavior would be still necessary.

The reinforcement orientation in MMCs, as one of those factors, had been studied by several researchers: Wang and Rack [7] observed that, for a $SiC_{p,w}$/7091Al composites at an applied load of 14.2 N, the run-in period wear rate depended upon the reinforcement orientation and the highest rate was with the perpendicular oriented SiC_w composite, and the steady state wear rate were generally independent of the reinforcement orientation (perpendicular vs. parallel); At a much higher load, 52 N, Pan *et al*. [8] concluded that the sliding wear rate of SiC_w/2124Al composites varied twofold in magnitude depending on orientation, the higher wear rate was found for the perpendicular-oriented SiC_w whereas the highest performance was for the parallel orientation which has the largest area fraction of whiskers; but Lee *et al.* [9] had found that the MMCs ($SiC_wAl_2O_{3f}$/6061) surface with reinforcements which were mostly normal to the wear surface had better wear resistance than the surface with the two dimensionally random orientation of reinforcements. All the studies mentioned above were carried on the discontinuously reinforced MMCs, and the dependence of tribological behavior on the orientation of reinforcements was still not clear.

Wear testing on the continuous ceramic fibre reinforced MMCs had only been reported by Greenfield *et al*. [10] with a found that: for the Al_2O_{3f}/Al-Li alloy composites, the antiparallel orientation results in the highest wear rate and the highest coefficient of friction; and the lowest wear rate and the greatest reduction of friction were usually observed with fibres that were normal to the surface and the direction of sliding. However, further studies are still necessary to identify the wear mechanism of this kind of MMCs.

The present works investigate the dependence of wear behavior of an Al_2O_3 continuous fibre reinforced Al-Cu alloy composites on fibres orientations. Apart from the three typical orientations (normal, parallel and antiparallel), other orientations—when fibres have 45 and 135 degree angle to sliding direction—will also be employed in this study. In particular, more attentions will be paid on fibres' fracture mechanism in each situation.

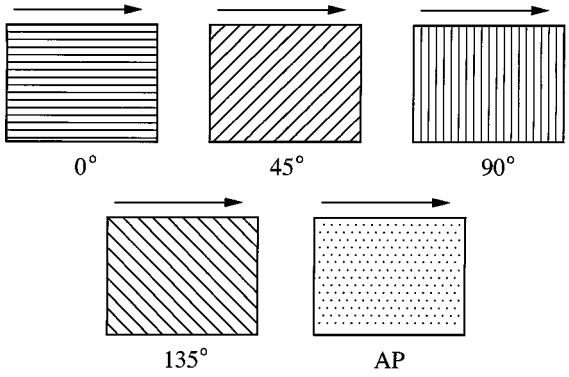

Figure 1 Orientations of fibres.

2. Experimental procedures

The MMCs studied in this work was alumina continuous fibre (γ-Al_2O_3, with a mean diameter of 17 μm) reinforced Al-4.43 wt%Cu alloy fabricated by a infiltration process described in detail in reference [11]. The wear test specimens were cut from the as-received composites, and the surface orientation were defined by comparing the fibre direction with respect to the direction of motion of the counterface. Fig. 1 pictures those five kinds of fibres' orientations: 0° orientation (or Parallel), fibres were parallel to the sliding direction; 45° orientation, fibres had an angle 45° to sliding direction; 90° orientation (or Normal), fibres were perpendicular to wear surface; 135°, fibres had an angle 135° to sliding direction; and AP orientation (or Antiparallel), fibres were parallel to wear surface and perpendicular to sliding direction. All specimens had a fibres' volume fraction about 0.55.

Sliding tests were carried out using a block-on-ring type of wear machine (OAT-U, Tokyo Testing Machine MFG Co. LTD.). The test system consists of a stationary MMC specimen ($10 \times 10 \times 2$ mm or $\phi 10 \times 2$ mm) mounted onto a specimen holder of $50 \times 30 \times 10$ mm, and a rotating steel ring (JIS-SUJ2 bearing steel) with an outside diameter of 30 mm, a inside diameter of 16 mm and a thickness of 3 mm heat treated to a hardness about HRC63. A normal load was applied through a loading arm during sliding tests, as sketched in Fig. 2.

Prior to wear testing, the wear surface of specimens were polished under water using silicon carbide papers from 180 to 600 grit, and the counterbody was trimmed by a grinder attached to the wear test machine, so that a line contact between the steel ring and the specimen was obtained. After this, both the specimen and the counterbody were cleaned by acetone.

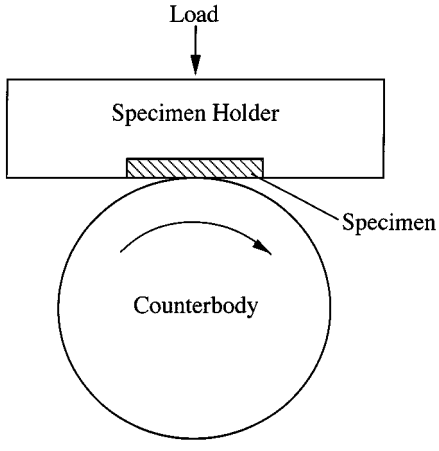

Figure 2 Composites specimen and the counterbody.

For each kind of specimens, the wear tests were undertaken at room temperature under following conditions: a constant normal pressure of 49 N, a constant sliding velocity of 0.94 m s^{-1}, and the sliding distance from 100 to 1800 m. Then the volume loss of composites specimens (ΔV) was calculated using:

$$\Delta V = B\left(r^2 \sin^{-1}\left(\frac{b}{2r}\right) - \frac{b}{2}\sqrt{\left(r^2 - \frac{b^2}{4}\right)}\right) \quad (1)$$

where B was the width of the sliding ring (3 mm), r was the radius of sliding ring ($r = D/2 = 15$ mm) and the b was the width of worn surface measured after wear testing.

Observations and analyses of the worn surface and subsurface were performed by a *Hitachi X-650* microanalyzer and an optical microscope, respectively. Debris produced from the wear tests were also analyzed.

3. Results and discussion

3.1. Wear results

The wear results for all the five kinds of orientations, expressed by volume loss vs. sliding distance, are plotted in Fig. 3. For the orientation of 45°, 90°, and 135°, the larger the fibres' angle is, the lower its volume loss is. The volume loss vs. sliding distance curves of these orientations have a similar slopes during the steady-state period. While in the case of 0° orientation, the

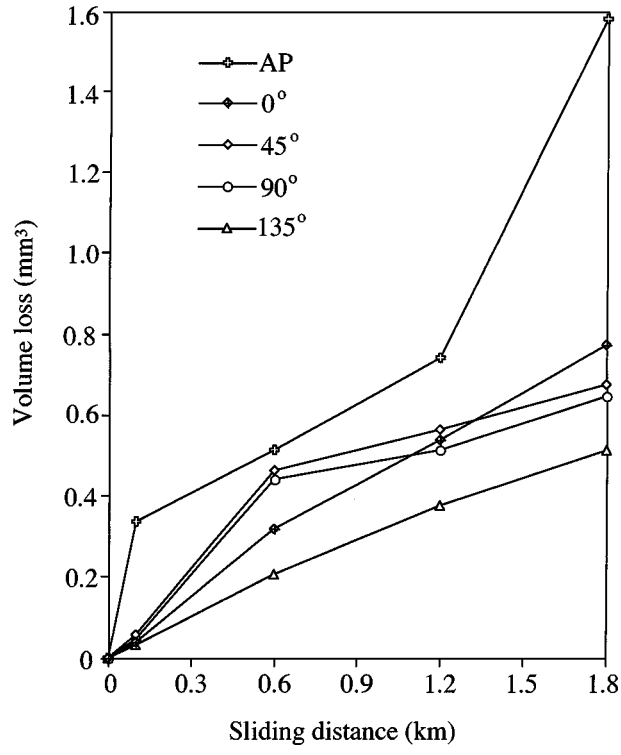

Figure 3 Volume loss vs. sliding distance curves for various orientations.

TABLE I Wear results of Al_2O_3/Al-4.43%Cu composites

Fibres orientation	Volume loss (mm^3)	Specific wear rate (10^{-6} mm^3/Nm)	Steady-state wear rate (10^{-4} mm^3/m)
0°	0.7723	8.757	3.802
45°	0.6775	7.682	1.790
90°	0.6477	7.343	1.735
135°	0.5114	5.799	2.567
Anti-parallel	1.5812	17.93	—

volume loss is greater than that of 135° orientation but less than those of the 45° and 90° orientations after a run-in period about 600 m, the slope of curve of this orientation is higher than those of the 45°, 90°, and 135° orientations, and its volume loss surpass those of the other orientations at a sliding distance of 1800 m. When the fibres are parallel to the wear surface and perpendicular to the sliding direction, the volume loss is greater than all of the other orientations at all sliding distances, indicating that fibres in AP orientation have the least resistance to sliding wear.

Three types of wear data, i.e., the total volume loss, the specific wear rate and the steady-state wear rate, were calculated and listed in Table I. Where the specific wear rate [8.10] is defined as the total volume loss (at a sliding distance of 1800 m) divided by the applied load times the sliding distance, and the steady-state wear rate [8] is calculated from the slope of the volume loss vs. sliding distance curve using the data after 600 m sliding wear. The 45°, 90°, and 135° orientations have their steady-state wear rate varying from 1.735×10^{-4} to 2.567×10^{-4} mm^3/m despite that their specific wear rates, which are 7.682×10^{-6}, 7.343×10^{-6} and 5.799×10^{-6} mm^3/Nm respectively, decrease with the increasing of fibre's angles. For the 0° orientation, both the specific wear rate (8.757×10^{-6} mm^3/Nm) and the steady-state wear rate (3.802×10^{-4} mm^3/m) are higher than those of the 45°, 90°, and 135° orientations. The curve of specific wear rate vs. fibres angle was plotted in Fig. 4 shows a decrease tendency within 0° to 135°. While, the specific wear rate of AP orientation (1.793×10^{-5} mm^3/Nm) are greater than all of the other orientations.

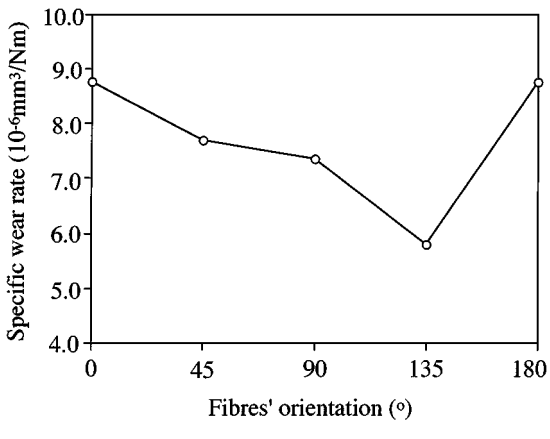

Figure 4 Specific wear rate vs. fibres' angle to sliding direction.

3.2. Wear morphology and debris analysis

Observations on the worn surface were performed by using scanning electron microscope (SEM) with a finding that all the worn surface are covered with a rough surface layer on which several fish-scale-like plateaus with a relative smoother surface are distributed. Those plateaus have a altitude difference with the rough surface on the side facing to the sliding direction but there is no obvious margins of these plateaus on the other side as representatively shown in Fig. 5. Cracks had been observed in the plateaus at the margin side facing the sliding direction at a higher amplification, shown in Fig. 6, indicating that these plateaus are always broken and then worn away at the side facing sliding direction and develop opposite to the sliding direction resulting a margin with a altitude difference. The electron probe microanalyser (EPMA) mapping of each element indicates that both the rough surface and the plateaus are consisted of transfer material from the counterbody and the fragmented materials from MMC itself. After been washed by acetone with the aid of ultrasonic, the broken fibres had been observed in a cave within the center of the worn surface (Fig. 7). Debris produced from wear

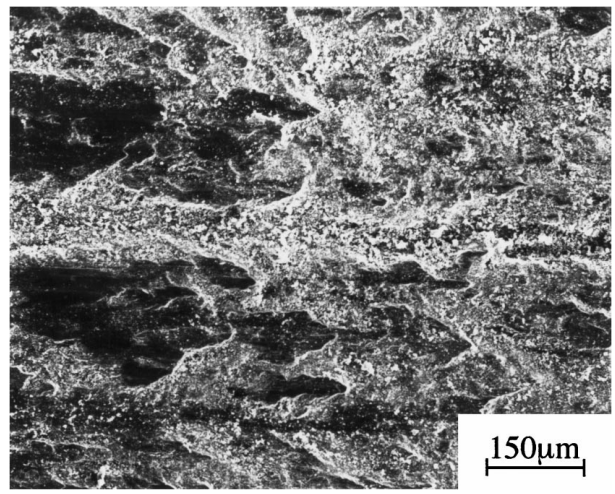

Figure 5 SEM micrographs of composite's worn surface of 0° orientation, 1800 m sliding, sliding direction is from left to right.

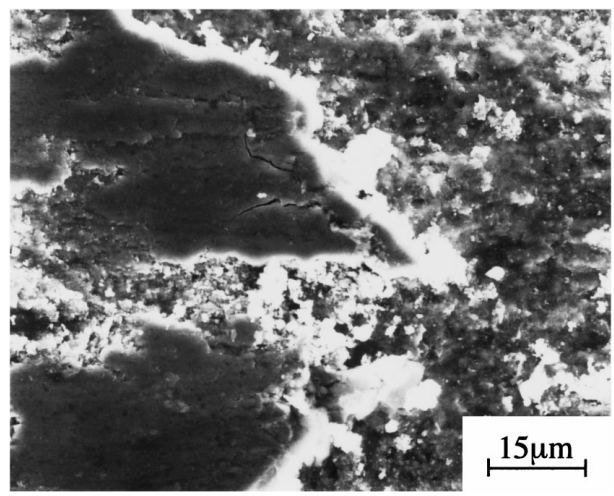

Figure 6 SEM micrographs of cracks generated on the worn surface of 0° orientation, 100 m sliding, sliding direction is from left to right.

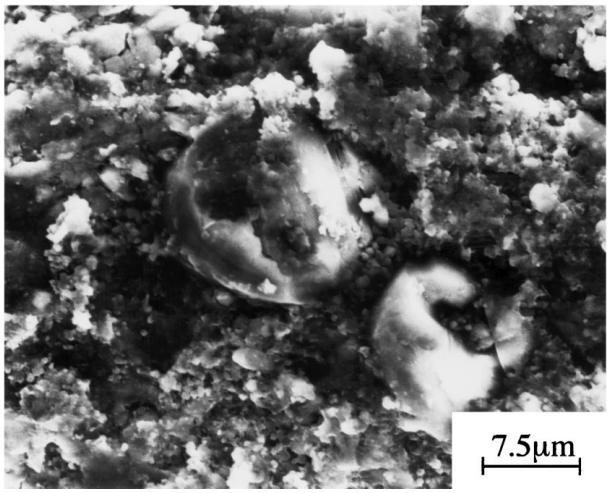

Figure 7 SEM micrographs of fibres fragment near the worn surface of 90° orientation, 100 m sliding, sliding direction is from left to right.

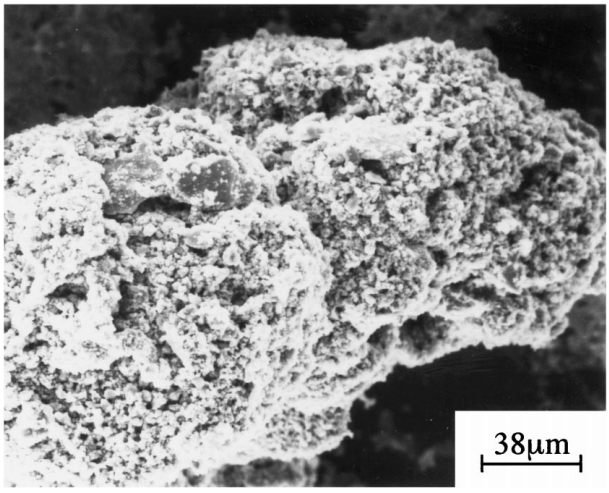

Figure 8 SEM micrographs wear debris collected from AP orientation after 1800 m sliding, sliding direction is from left to right.

process take a form of particles clusters with disparity sizes, they had been deformed during their moving from the delamination position to the boundary of worn surface. Micro observation and EPMA mapping show that both the surface morphology and the constitution of the debris are similar to those of the rough part of worn surface. A SEM micrographs of debris is given in Fig. 8.

3.3. Observation of worn subsurface

Fig. 9 are optical micrographs of composites' cross section through their worn surface and parallel to sliding direction after 100 m sliding wear. In the 0° orientation specimen (Fig. 9a), fibres near the worn surface were broken and the fragments generally stay in their original positions, no obvious deformation layer can be observed in this section. While in the case of 45°, 90°, and 135° orientation (shown in Fig. 9b, c and d, respectively), fibres within certain depth below the worn surface were broken, and fibres chops tend to align with the sliding direction. The movement of fragments indicates that the composites had been suffered the plastic deformation before they were worn away from the surface. In addition, fine fragments (with a sizes smaller than the fibres' diameter) are found in the place very near the worn surfaces. The subsurface morphology of composites after 1800 m sliding wear have been observed to be similar to those after 100 m sliding's.

3.4. Wear mechanism

All the five kinds of composites specimens had a similar worn surface morphology. According to the results from above observations, the worn mechanism of the surface layer is inferred as follows: At first, the surfaces are made to conform to each other, the matrix is easy to be deformed and so the load is mainly supported by the fibres and/or their fragments, and a real area of contact is established. The composites surface are mainly consisted of broken fibres and the matrix alloy covered with a thin alumina film due to oxidations. As a result of relative motion, Fe-rich material is transferred from the counterface to composites surface due to the micro-grooving of the alumina fibres and the alumina film. The transferred materials are oxidized before and/or after they attach to composites' worn surface. From here, a kind of small nuclei of oxides plateaus are formed at the spots of the real area of contact due to oxidation of all major metallic elements both in the MMC and from the counterbody, and the oxidation process is enhanced by friction heating. During this period, the submicron oxides would be embedded into the Al alloy matrix by the external forces forming a complicated mixture. These plateaus grow in height to a critical thickness and protrude above the surrounding surface areas. Due to surface fatigue and the repeated plastic deformation by the counterbody, micro cracks are generated in oxide plateaus. These cracks develops and the oxide plateaus breaks up opposite to the sliding direction to form flakes and/or small debris. The plateaus are mainly supported by the underlying fibres, and the broken fibres are further more pulverized into fine pieces during the growth and peeling off of the plateaus. After removal of the elevated oxide plateaus, other load-bearing plateaus are formed and the oxidation and micro-grooving processes continuous. The metallic debris produced will be deformed and fractured during sliding, which increases its surface exposed to the environment. Thus metallic debris is easily oxidized, even at low ambient temperatures. Oxide debris of submicron size crystals can be agglomerated to form debris clusters on the boundary of worn surface.

4. Discussions on the influence of fibres' orientation on wear

Although the wear mechanism of surface layer are similar for all specimens, the wear results are related obviously to fibres' orientations. We contribute it to the difference of fibres' broke mechanism and subsurfaces' deformation in each kind of situations as detail discussed in the following:

1) *In the case of 45°, 90°, and 135° orientations.* Many factors could influence the wear mechanism

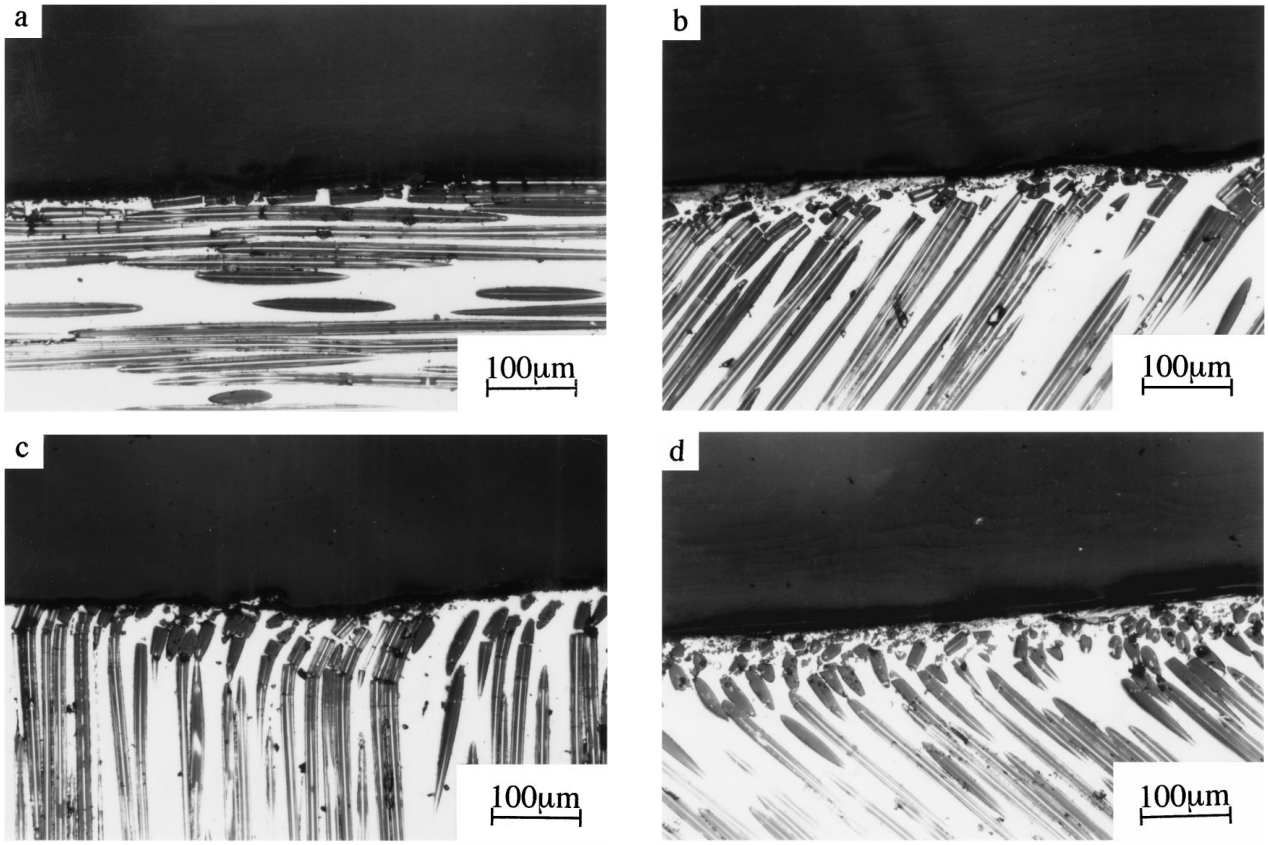

Figure 9 Optical micrographs of composites' cross section through their worn surface and parallel to sliding direction. (a) 0° orientation, (b) 45° orientation, (c) 90° orientation and (d) 135° orientation, sliding direction is from left to right.

during sliding contact [12]. It is reasonable to propose that, during the run-in period, fibre fracture is a controlling step in the wear of continuously reinforced MMCs. Fibre fracture can occur where there is an unsupported length. Loss of support can result from the chipping or wearing away of the matrix from around the fibres or by softening of the matrix, leaving the fibre as a cantilevered beam [13]. In the present studies, specimens are the hard ceramic fibre reinforced soft matrix MMC, under the adhesive effect, the matrix have a tendency to flow in the sliding direction leaving fibres to support the load and the friction force. For a quantitative analysis, fibres in above conditions can be simply considered as a beam with axial loads, then the stress in it is,

$$\sigma = N/A + My/I \tag{2}$$

where: N is axial force, A is area of cross section, M is bending moment, y is the distance to beam central, and I is moment of inertia.

In present studies, fibres have an angle (θ) to sliding direction, and are subjected to a normal press P(N/m^2, perpendicular to wear surface) and a tangenital friction force μP(N/m^2, parallel to sliding direction) as illustrated in Fig. 10, so the axial force F_x and lateral force F_y at the end of this fibre are:

$$F_x = \pi d^2 P(\mu ctg\theta - 1)/4 \tag{3}$$

$$F_y = \pi d^2 P(ctg\theta + \mu)/4 \tag{4}$$

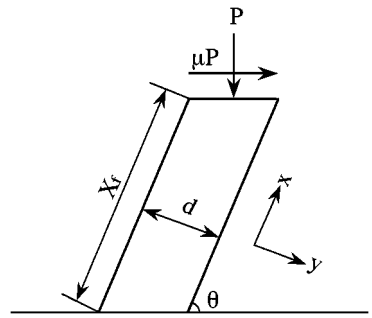

Figure 10 Schematic diagram for the stress analysis of fibres in the worn subsurface.

where d is diameter of fibre. For Equation 2, there are following relations:

$$A = \pi d^2/4 \tag{5}$$

$$I = \pi d^4/64 \tag{6}$$

$$N = F_x = \pi d^2 P(\mu ctg\theta - 1)/4 \tag{7}$$

$$M = F_y X_f = \pi d^2 P X_f (ctg\theta + \mu)/4 \tag{8}$$

where X_f is the length of fibre beam. And for the maximum stress

$$y = d/2 \tag{9}$$

Substituting Equation 5 to Equation 9 into Equation 2, yields

$$\sigma = P[(\mu ctg\theta - 1) + 8X_f(ctg\theta + \mu)/d] \quad (10)$$

this reveals the largest tensile stress occurs at the bottom of the fibre beam. Obviously, the fibres orientation has a great influence on the maximum stress, and the stress values for the various orientations are given as follows:

$$\sigma_{45} = P[(\mu - 1) + 8X_f(\mu + 1)/d] \quad (11)$$

$$\sigma_{90} = P[-1 + 8X_f\mu/d] \quad (12)$$

$$\sigma_{135} = P[-(\mu + 1) + 8X_f(\mu - 1)/d] \quad (13)$$

Here $\sigma_{45} > \sigma_{90} > \sigma_{135}$ indicating that fibres normal to the wear surface are easier to be broken than those having the angle 135° to the sliding direction, but they are better than those distributed in 45° orientation. The above qualitative analysis are correspond to the experimental results obtained from subsurface observations except that fibres in the center part of worn surface are easily to be broken than those near the worn boundary. With the development of worn surface, the normal press per unit worn surface area are gradually decreased, this in turn would also affect the wear mechanisms, but no obvious change in wear mechanism was observed under the present testing conditions.

After been broken, fibres' chops are flowed with the matrix's deformation and tend to align their axes with the sliding direction. It is the obstruction behavior of fibres' fragment that enhances the wear resistance of surface layer, because the deformation of subsurface will undoubtedly accelerate the fracture of oxide-plateaus. Among the three kinds of orientations (45°, 90°, and 135°), the 45° orientations results in the smallest angle between fibres' axes and the sliding direction, and so the fragments only do a relatively little resistance to matrix's deformation before they are worn away from the composites' blocks. While in the case of 135° orientations, fragments have to long march (or turn a large angle) to align their axes to the sliding direction (Fig. 9d), so they have enough time to give full play to their resistance behavior to the matrix's deformation. The case of 90° orientation's situated between those of 45° and 135° orientation's. For the consideration of fragments' resistance behavior to the deformation of subsurface layer, the larger angle is beneficial to composites' wear resistance.

2) *In the case of 0° orientation.* Different from the cases of 45°, 90°, and 135° orientations in which fibres are sequentially broken along their axial, fibres in the 0° orientation specimen bear the normal press and act as the "simple beams," and so, they are broken at the same step (Fig. 9a). Fibres' broken can also spread to the outer of worn surface as a evidence given in Fig. 11 showing that fibres in the un-worn surface had also been broken at the end near the worn boundary. Fibres on the worn surface are parallel to sliding direction that would have less resistance to the sliding of counterbody. Once they are broken, the fragments are easily moved and worn away, and so the plastic deformation layer is very thin in this plain distributed situation. Layer by layer, the worn surface is rapidly developed into composites blocks. Fibres' layer-style-broken and the fragments' little resistance make the 0° orientation to have a steady-state wear rate greater than those in the 45°, 90°, and 135° orientations.

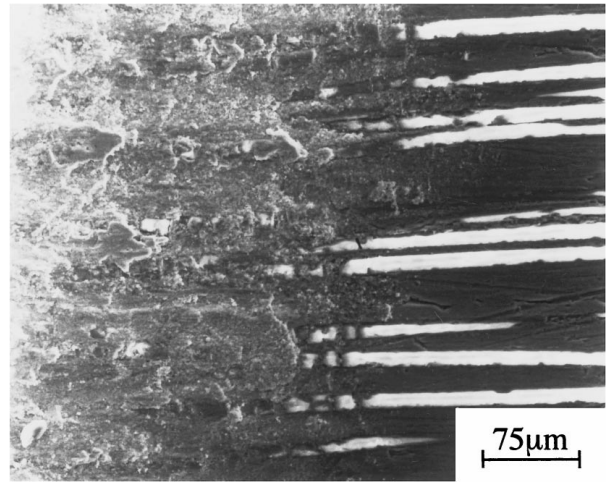

Figure 11 SEM micrographs of the boundary region of worn surface showing the fibres broken near this boundary, 0° orientation, 100 m sliding, sliding direction is from left to right.

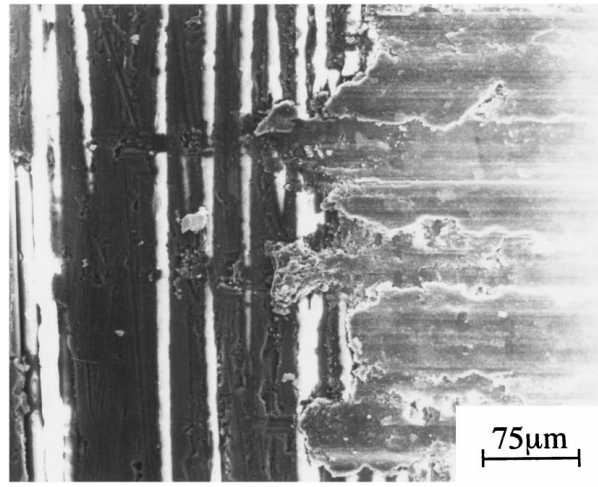

Figure 12 SEM micrographs of the boundary of worn surface showing the fibres received abrasion by the rough counterface, AP orientation, 100 m sliding, sliding direction is from left to right.

3) *In the case of AP orientation.* Apart from their plain distribution which would result a higher wear rate, fibres in anti-parallel orientation can be more easily broken and worn away than those in the case of 0° orientation, due to that a rough counterface will obviously aggravate the fraction of fibres distributed cross the sliding direction, as the Fig. 12 shows that fibres had been abrasion worn by the micro points protrude on the counterface. If the roughness of counterface is larger than fibres' diameter, this lateral-abrasion effect would became more serious. So the AP orientation has the least wear resistance.

5. Summary

The wear behavior of Al_2O_3 continuous fibre reinforced Al-4.43%Cu composites against a steel counterface in a dry sliding conditions depends strongly on the fibres orientations: for the 45°, 90°, and 135° orientations, the larger the fibers' angle was, the lower the

composites' volume loss were; and the 0° orientation resulted a higher steady-state wear rate than those of the 45°, 90°, and 135° orientations; when fibres were anti-parallel the sliding direction, the largest wear rate had been observed at all sliding distances.

Dominant wear mechanism was suggested from wear surface analyses. The major wear mechanism was inferred as a oxidation-microgrooving process, i.e. under the micro-grooving behavior of the alumina fibres and the alumina film, metal materials were transferred into the worn surface to form oxide-plateaus with fibres' fragments and the composites' matrix. The wear rate of composites' were mainly determined by the formation and fracture of these oxide-plateaus.

The influence of fibres' orientation on composites' wear resistance was revealed from the observation of worn subsurface and the fibres' stress analyses in the fibres. For the 45°, 90°, and 135° orientations, the smaller orientation angle resulted a greater stress in fibres, and also the fibres' broken fragments had less resistance to the deformation of worn subsurface, these resulted a less wear resistance. In the case of 0° and AP orientations, fibres were plain-layer distributed, and were easily broken and worn away, these in turn, decreased composites' wear resistance. In addition, the wear rate in AP orientation would be raised by the roughness of counterface.

Acknowledgement

We would like to express our thanks to Dr. N. Nakamura for his allowing the use of wear testing machine, thanks are also to Mr. Wakasugi for his helping operate the scanning electronic microscope.

References

1. T. DONOMOTO, N. MIURA, K. FUNATANI and N. MIYAKE, SAE Technical Paper, No. 83052, 1983.
2. M. FUJINE, T. KANEKO and J. OKIJMA, *JSAE Rev.* **14**(3) (1993) 48–52.
3. T. HAYASHI, H. USHIO and M. EBISAWA, SAE Technical Paper, No. 890557, 1989.
4. M. EBISAWA, T. HARA, T. HAYASHI and H. USHIO, SAE Technical Paper, No. 910835, 1991.
5. T. SUENAGA, *IMONO* **64** (1992) 881–886.
6. A. P. SANNINO and H. J. RACK, *Wear* **189** (1995) 1–19.
7. A. WANG and H. J. RACK, *Mater. Sci. Eng.* **A147** (1991) 211–224.
8. Y. M. PAN, M. E. FINE and H. S. CHENG, *Tribol. Trans.* **35** (1992) 482–490.
9. C. S. LEE, Y. H. KIM, K. S. HAN and T. LIM, *J. Mater. Sci.* **27** (1992) 793–800.
10. I. G. GREENFIELD and R. R. VIGNAUD, in Advanced composites: Proceeding (ASM, Metal park, OH, 1985) pp. 213–221.
11. H. N. LIU, H. MIYAHARA and K. OGI, *Mater. Sci. Tech.* **4** (1998) 292.
12. K.-H. ZUM GAHR, "Microstructure and wear of materials" (Elsevier Science Publishing Company Inc. 1987) pp. 351–477.
13. J. M. MCKITTRICK, N. S. SRIDHARAN and M. F. AMATEAU, *Wear* **96** (1984) 285–299.
14. GERE and TIMOSHENKO, "Mechanics of materials," 3rd SI ed. (Chapman & Hall, 1991) pp. 292–294.

Received 19 October 1997
and accepted 3 June 1999